Pre-operative simulation of post-operative multifocal vision

Maria Vinas,[1,*] **Sara Aissati,**[2] **Mercedes Romero,**[1] **Clara Benedi-Garcia,**[1] **Nuria Garzon,**[2] **Francisco Poyales,**[2] **Carlos Dorronsoro,**[1] **and Susana Marcos**[1]

[1]*Institute of Optics, Spanish National Research Council, IO-CSIC, Serrano, 121, Madrid 28006, Spain*
[2]*IOA Madrid Innova Ocular, Madrid, Spain*
*maria.vinas@csic.es

Abstract: While multifocal intraocular lenses (MIOLs) are increasingly implanted to correct for presbyopia, how one sees with a multifocal correction is hard to explain and imagine. The current study evaluates the quality of various visual simulating technologies by comparing vision with simulated MIOLs pre-operatively and the implanted MIOLs post-operatively in the same patients. Two simulation platforms were used: (1) a custom-developed adaptiveoptics (AO) system, with two visual simulator devices: a spatial light modulator (SLM) and an optotunable lens operating under temporal multiplexing (SimVis); and (2) a wearable, binocular, large field of view SimVis2Eyes clinical simulator (SimVis Gekko, 2Eyes Vision, Madrid, Spain). All devices were programmed to simulate a trifocal diffractive MIOL (POD F, FineVision, PhysIOL). Eight patients were measured pre-operatively simulating the trifocal lens and post-operatively with implantation of the same MIOL. Through-focus decimal visual acuity (TF VA) was measured (1) monocularly in monochromatic light using a four-alternative-forced-choice procedure in the AO system; and (2) binocularly using a clinical optotype in white light. Visual simulations pre-operatively predict well the TF VA performance found post-operatively in patients implanted with the real IOL. The average RMS difference between TF curves with the different visual simulators was 0.05 ± 0.01. The average RMS difference between the TF VA curves with the SimVis pre-operatively and the real MIOL post-operatively was 0.06 ± 0.01 in both platforms, and it was higher in cataract eyes (0.08 ± 0.01, on average across simulators) than in eyes with clear lens. In either group the shape of the TF curves is similar across simulators and pre- and post-operatively. TF curves cross-correlated significantly between simulators (lag $k = 0$, rho $= 0.889$), as well as with results with the real MIOL implanted (lag $k = 0$, rho $= 0.853$). Visual simulations are useful programmable tools to predict visual performance with MIOLs, both in an AO environment and in a clinical simulator. Pre-operative visual simulations and post-operative data are in good agreement.

1. Introduction

Multifocal corrections work under the principle of simultaneous vision, projecting simultaneously focused and defocused images on the retina, providing multifocality at the expense of reducing optical quality at all distances [1]. Visual simulators are proposed to provide patients the visual experience of a multifocal correction before this is applied to the eye (either in the form of intraocular lens, IOL, or contact lens, CL). However, to our knowledge, their capability to replicate real clinical corrections in real individual patients has not been fully demonstrated.

Visual simulators based on Adaptive Optics (AO) have allowed probing the visual system under manipulated optics [2–5]. They are particularly attractive to test vision in patients with new optical designs [2,6,7] prior to delivering surgical corrections to the patient or even manufacturing the lenses. Simulations of new corrections with AO primarily serve to investigate interactions between the patient's optics and a given correction, to investigate differences across corrections,

and eventually to select the correction that optimizes perceived visual quality and performance in patients [2,6,8].

In AO-based visual simulators, an active optical element (deformable mirror, spatial light modulator or optotunable lens) reproduces the equivalent phase map of a certain optical design in a plane conjugate to the subject's pupil plane, while the observer is looking at a visual stimulus. Deformable Mirrors (DM) allow inducing aberrations [9,10], or simulating smooth optical designs [11,12], while controlling the aberrations of the subject [13]. On the other hand, spatial light modulators (SLMs) [2,7,14,15], generally liquid crystal-based on silicon (LCoS)-SLMs devices, are capable of reproducing abrupt phase maps due to their high spatial resolution, and to increase the effective phase range through the use of wrapped phase representations [16,17]. Previous work has evaluated perceived visual quality at various distances with presbyopic corrections simulated in AO systems: multifocal angular and radially segmented corrections [2,6], corneal inlays [18] or diffractive optics [19,20]. A different approach is to place the real IOL in a cuvette in a conjugate pupil plane projected in the eye, although in this case, simulations are limited by the static nature of this approach [21]. To date most visual simulations have been limited to experimental environments [22,23], given the relatively high complexity and large foot-print of the simulators, although some have made their way into commercial products [7,16,24]. In these on-bench or desktop-based devices [25] the visual experience is limited to stimuli projected in a mini-display subtending a relatively small visual field, in many cases monocularly.

In order to increase the accessibility of visual simulations in the clinic, we have recently developed SimVis technology [8,26] for simultaneous vision simulation, using optotunable lenses working in a temporal multiplexing mode, i,e, scanning multiple foci to provide superimposed images on the retina, all of them with the same position and magnification, but corresponding to different planes in focus. The simulation of multifocal corrections relies on evaluating the through-focus (TF) energy distribution of the correction, from the knowledge of the spatially varying pupillary power distribution, and programming in the optotunable lens the corresponding time-varying focus changes. The simulated multifocal correction is tuned to match the TF optical quality (in terms of Visual Strehl) [27] of real existing multifocal lenses [26].

In a previous study, we compared TF optical and visual quality produced by real MIOLs in a cuvette projected on the subject's eye with those same designs simulated with SimVis technology and with a Spatial Light Modulator (SLM), incorporated in a custom-made multichannel 3-active-optical-elements polychromatic AO Visual Simulator, and we found good correspondence between performance of the real and simulated MIOLs. A wearable clinical visual simulator (SimVis Gekko, 2Eyes Vision, Madrid, Spain) has now been developed for the pre-surgical simulation of presbyopic corrections based on the SimVis principle. This new device is binocular, see-through, allows a direct view of the real world and has a larger visual field.

The current study evaluates visual simulation of MIOLs using 2 different simulation technologies (SLM and SimVis technology) in patients before and after implantation of commercial diffractive trifocal lenses using two simulation platforms, an AO-based visual simulator and the clinical visual simulator, SimVis Gekko.

2. Methods

TF Visual Acuity (TF VA) was measured in eight subjects, five with clear crystalline lens and 3 with some degree of cataract, pre-operatively through simulated MIOLs, using 2 different visual simulators, and post-operatively, after bilateral implantation of the same MIOL.

2.1. Multifocal IOL

The simulated and later implanted lens was a trifocal diffractive IOL, the FineVision POD F (PhysIOL, Liège, Belgium), a hydrophilic (26% hydrophilic acrylic) aspheric multifocal diffractive IOL built with a combination of two bifocal diffractive patterns, one for far and

near-vision and the other for far and intermediate-vision [28,29]. The combination of the two diffractive structures provides 3 useful focal distances: 0.0 D for far-vision, +1.75 D addition for intermediate-vision and + 3.50 D addition for near-vision [23,30].

2.2. Patients and surgery

The study was conducted on eight presbyopic patients (mean age: 60.4 ± 7.7 years; range: 53 to 74 years): five of them with clear lens and three with different cataract grades. Measurements were performed pre-operatively (5 days before IOL implantation, on average) and post-operatively (30 days after IOL implantation, on average). All participants were acquainted with the nature and possible consequences of the study and provided written informed consent. All protocols met the tenets of the Declaration of Helsinki and had been previously approved by the Spanish National Research Council (CSIC) Bioethical Committee.

Patients received a complete ophthalmic evaluation prior to enrollment in the study and surgery at IOA Madrid Innova Ocular (Madrid, Spain). Table 1 summarizes all pre- and post- operative data of the patients, indicating the instrumentation used for each measurement. The participating patients had already been scheduled for implantation of a trifocal diffractive IOL and their inclusion in the study did not affect any surgical parameter. The inclusion criteria for the study were: good general health, no ocular pathology, no previous ocular surgery, required IOL power between 16 and 26 D, and corneal astigmatism less than 1.25 D. Patients with diplopia (double vision) were excluded from the experiment. Patients were bilaterally implanted with the trifocal diffractive IOL, with a time difference of less than 7 days between surgeries in each eye. The required IOL power was computed with Barrett II Universal formula. The target refraction was emmetropia. Natural pupil of the subjects was in all cases higher than 4 mm.

All surgical procedures were performed by the same experienced surgeon (FP) under topical anesthesia and aided by a computer-assisted cataract surgery system (CALLISTO eye, Zeiss Cataract Suite Markerless; Carl Zeiss, Jena, Germany). IOLs were implanted through a 2.2-mm self-sealing clear corneal incision at 180 degrees (temporal) in right eyes and at 90 degrees (superior) in left eyes and about 1 mm anterior to the limbus. A femtosecond laser (CATALYS Precision Laser System, Abbott Medical Optics Inc., Santa Ana, CA, USA) was used to perform the anterior capsulotomy (5-mm diameter) as well as lens fragmentation. The selected IOL was then implanted in the capsular bag with a single-use injection system (Accujet, Medicel, Thal, Switzerland). A capsular tension ring (CTR) was inserted in all eyes, followed by ophthalmic viscoelastic traces removal.

2.3. Visual simulation platforms

Two visual simulation platforms were used to perform the measurements before and after implantation of the MIOLs: (1) a multichannel AO-based visual simulator, which incorporates a spatial light modulator (SLM) and a simultaneous vision simulator (SimVis) based on temporal multiplexing of an opto-tunable lens, and (2) a SimVis2Eyes visual simulator, as described in Fig. 1.

2.3.1. Visual simulation platform1: AO-based visual simulator

Visual tests were performed in a custom-developed *multichannel polychromatic AO system* (Fig. 1(A), left) at the Visual Optics and Biophotonics Lab (IO-CSIC, Madrid, Spain). The main components of the system are described in detail in previous publications [2,5,6,23]. In the current study, the visual stimulus in the AO system is seen through different active optical elements in 3 separate channels: (1) a reflective deformable mirror (DM), used in this study to correct the system aberrations; (2) a reflective phase-only spatial light modulator (LCoS-SLM), and (3) a simultaneous vision simulator (SimVis) based on temporal multiplexing of an opto-tunable lens, both used to simulate the multifocal designs. The MIOL design was mapped in the SLM (as

Table 1. Pre- and post-operative clinical data of the patients of the study. M and F stand for male/female, respectively; age in years; R and L stand for measured right eye/left eye; [1]refractive error: Sph, spherical error; Cyl (Diopters), cylinder (Diopters); Axis(degrees); [2]BCVA, Best Corrected Visual Acuity and UCVA, Uncorrected Visual Acuity, measured under photopic lighting conditions with ETDRS (Early Treatment Diabetic Retinopathy Study, ETDRS; Precision Vision, Woodstock, IL, USA) chart; [3]Cataract grade (according to BCN 10 grading system [31], using frontal and cross-sectional slit-lamp lens images, ranging from N0 (clear lens) to N10 (dark lens); Prelex stands for Presbyopia Lens Exchange (clear lens). Shading indicates measured eye for each patient.

Pre-operative data

Subject/ Sex	Age	Eye	Sph[1]	Cyl[1]	Axis[1]	BCVA[1]	Cataract[3] grade	Days before surgery
S#1/F	70	RE	3.25	0	-	0.7	N3	4
		LE	3.75	0	-	0.9	N3	
S#2/M	60	RE	2	0	-	1	N1+ subcaps post	3
		LE	2.25	0	-	0.8	N1 + subcaps post	10
S#3/F	57	RE	0.75	−0.5	10	1	Prelex	3
		LE	1	−0.5	145	1	Prelex	
S#4/M	53	RE	2.5	−0.5	30	1	Prelex	6
		LE	2.5	−0.5	20	1	Prelex	
S#5/F	54	RE	1	−0.5	165	1	Prelex	3
		LE	0.75	0	-	1	Prelex	
S#6/M	74	RE	1.75	0	-	1	N4	1
		LE	1.75	−0.5	80	1	N3	
S#7/F	55	RE	1.5	−0.5	80	1	Prelex	5
		LE	2.75	−0.5	80	1	Prelex	4
S#8/F	60	RE	1	−0.5	140	1	Prelex	7
		LE	0.5	0	-	1	Prelex	2

Post-operative data

| Subject/ Sex	Age	Eye	IOL power (D)	Sph[1]	Cyl[1]	Axis[1]	UCVA[1]	BCVA[1]	Days after surgery
S#1/F	70	RE	25.5	−0.25	0	0	0.95	1	24
		LE	26	0	0	0	0.76	0.76	
S#2/M	60	RE	22.5	0	−0.50	120	0.76	0.95	10
		LE	22.5	0	−0.50	65	0.72	1	3
S#3/F	57	RE	22	0	0	0	1	1	7
		LE	22.5	0	0	0	1	1	
S#4/M	53	RE	23.5	1.00	−0.75	170	0.72	1	7
		LE	23.5	0.5	0	0	0.8	1	
S#5/F	54	RE	24.5	0	0	0	0.95	0.95	13
		LE	24.5	0	0	0	0.95	0.95	
S#6/M	74	RE	21.5	0	0	0	1	1	8
		LE	21	0	0	0	1	1	
S#7/F	55	RE	23	−0.25	−0.50	105	0.8	1	6
		LE	25	0	0	0	1	1	8
S#8/F	60	RE	21	0	0	0	1	1	10
		LE	21.5	0	0	0	1	1	15
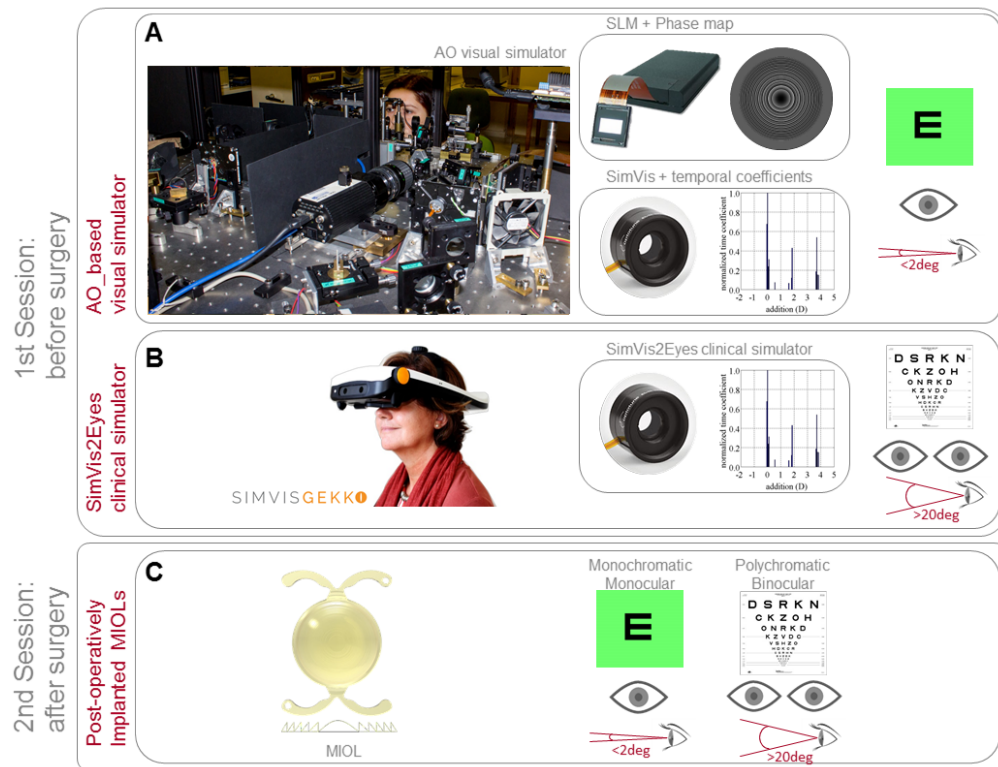
Fig. 1. Visual simulation platforms. (A) AO-based visual simulator incorporating the SLM and SimVis in the corresponding conjugate pupil planes of the AO system. MIOL was simulated using a phase map and time coefficients for the SLM and SimVis, respectively. Measurements were performed monocularly at 555 nm. (B) SimVis2Eyes_clinical visual simulator based on SimVis technology, using time coefficients, working binocularly and with the stimulus in white light. (C) MIOL implanted in the eight patients. Post-operatively, measurements were performed monocularly (using a monochromatically illuminated green target projected in a DLP projector subtending a 1.62-deg field in an AO system) and binocularly in white light (ETDRS target at distance, subtending a 20 deg field).

a spatial phase map) [23,26] and on the SimVis (as a temporal profile) [25,29], as shown in Fig. 1(A).

The channels of the AO system used in the current study include (1) an *Illumination-Channel*, containing a supercontinuum laser source (SCLS, Fianium Ltd, United Kingdom) with selectable wavelengths (555 nm for illumination of the target stimulus and 827 nm for aberration control, in the current study), coming out from two independent fiber-channels; (2) an *AO-Channel* consisting of a Hartmann-Shack wavefront sensor (HASO 32 OEM, Imagine Eyes, France) and an electromagnetic deformable mirror (DM) (MIRAO52, Imagine Eyes, France), allows measurement and correction of the system aberrations, respectively; (3) an *SLM-Channel* consisting of a reflective phase-only LCoS-SLM (SLM; VIS; Holoeye Photonics AG, Germany), used to generate the multifocal phase designs; (4) a *SimVis-Channel*, consisting on an optotunable lens (EL-10-30-C, Optotune Inc., Switzerland) working on temporal multiplexing mode (SimVis). The DM, SLM, and SimVis were placed in conjugate pupil planes of the system. The MIOL design was mapped in the SLM (as a spatial phase map) and on the SimVis (as a temporal profile), as shown in Fig. 1(A). The system also incorporates; (5) a *psychophysical-Channel* consisting of a Digital Micro-Mirror Device (DMD) (DLP Discovery 4100 0.7 XGA, Texas Instruments, USA),

placed in a conjugate retinal plane, and used to display visual stimuli with a 1.62 deg angular subtend. The DMD is monochromatically illuminated with light coming from the SCLS, 555 nm in this experiment; (6) a *pupil monitoring-Channel* consists of a camera (DCC1545M, Thorlabs GmbH, Germany) conjugated to the eye's pupil, and (7) a *Badal optometer-Channel* corrects for defocus in AO-, SLM-, Testing- and Psychophysical-Channels and allows TF psychophysical testing. Two automatized shutters allow simultaneous illumination of the eye and the stimulus.

SLM   The diffractive multifocal component of the trifocal diffractive IOL was mapped onto a reflective phase-only LCoS-SLM, while the refractive component was adjusted with the Badal Optometer. The procedure to generate a multifocal phase map has been described in previous publications. In particular, the trifocal diffractive IOL was obtained, tested and validated in a prior work from our group [23].

In brief, the multifocal phase maps of the trifocal diffractive IOL was extracted in pseudophakic computer eye models from the knowledge of the surface height profiles of the lenses, provided by the manufacturer, as described in a previous publication [32]. The SLM addressable phase map was first evaluated from the multifocal phase map and later 2π-wrapped, so that the generated phase pattern was a grey-scale image, where each level of grey corresponds to a certain phase difference in the interval $[0\ 2\pi]$. Phase-maps (Fig. 1(A)) were programmed for 4-mm pupil diameters and 555 nm wavelength.

SimVis   The diffractive multifocal component of the trifocal diffractive IOL was also mapped onto the Simultaneous Vision Simulator (SimVis), consisting on an opto-mechanically tunable lens (EL-10-30-C, Optotune Inc., Switzerland), operating under temporal multiplexing mode [8,26]. The tunable lens scans multiple foci to provide superimposed images on the retina, all of them with the same position and magnification, but corresponding to different planes of focus. As the temporal frequency is higher than the flicker frequency of the human visual system, the retinal image is perceived as a static multifocal image.

The simulated multifocal correction is tuned to match the through-focus optical quality (in terms of Visual Strehl [27]) of real multifocal lenses. It is an iterative optimization of the electrical input signal driving the lens and, consequently, of the SimVis through-focus optical quality [26]. In particular, the temporal profile [32] that describes the trifocal diffractive IOL was obtained, tested and validated in previous work [23]. The tunable lens of the SimVis was placed in an additional conjugate pupil plane. The time coefficients of the input signal were calculated for 4-mm pupil diameters and 555 nm wavelength (Fig. 1(A), bottom).

2.3.2.   Visual simulation platform2: SimVis2Eyes clinical visual simulator

In this study, we also used the SimVis technology in a second simulation clinical platform (SimVis Gekko, Fig. 1B, left) In this binocular wearable device, a couple of relay lenses project the tunable lens (EL-10-30-C, Optotune Inc., Switzerland) onto the patient's pupil. The device is based on a previous see-through monocular prototype [33], but incorporates now binocular vision with a wider field of view (20°). The device has wireless operation and allows observation of the real world with a multifocal correction. Both SimVis (Platform 1) and SimVis2Eyes (Platform 2), use the same temporal multiplexing technology, and the same time coefficients to simulate the multifocal lens. The measurements in Platform 2 are binocular, and are performed with white light with a clinical optotype (see section Visual tests & experimental protocol).

2.4. Visual test & experimental protocol

2.4.1. Through-focus Visual Acuity in the AO-based visual simulator

For the visual simulator Platform 1 (AO system), TF VA was measured using an 4-Alternative Forced Choice (4AFC) [34] procedure with Tumbling E letters and a QUEST (Quick Estimation by Sequential Testing) algorithm programmed using Psychtoolbox [35]. The stimulus was projected in the Digital Micro-Mirror Device (DMD), illuminated monochromatically at 555 nm (>20 cd/m^2 with both, SLM and SimVis, measured at the retinal plane of the system). The QUEST routine for each VA measurement consisted of 40 trials, each one presented for 0.5 seconds, where the threshold criterion was set to 75%. The threshold (VA) was estimated from the average of the 10 last E-letter stimulus size values. VA was expressed in terms of decimal acuity (logMAR = -log$_{10}$[decimal acuity]) [36].

   Measurements were performed monocularly, in a darkened room. Patients were stabilized using a dental impression and the eye's pupil was aligned to the optical axis of the instrument (using an x-y-z stage moving a bite bar) using the line of sight as a reference, while the natural pupil is monitored using a pupil camera. To ensure constant pupil diameter during the measurements, a 4-mm artificial pupil was placed in a conjugate pupil plane.

   The patients were instructed on the nature of the experiment and performed some trial runs prior to the test. They were asked to adjust the Badal system position to achieve best subjective focus. Through-focus measurements were obtained changing vergences with the Badal optometer ranging from -1.00 to + 4.00 D. TF VA was measured in the AO system pre-operatively monocularly, in one eye, (Session 1, with the MIOL simulated either with the SLM or the SimVis -in a random order-) and post-operatively (without any simulator element) monocularly in the same eye.

2.4.2. Through-focus Visual Acuity in the SimVis2Eyes clinical visual simulator

For the visual simulator Platform 2 (SimVis2Eyes, the binocular wearable device), VA was measured binocularly using a standard high contrast ETDRS clinical optotype in photopic lighting conditions (≈85 cd/m^2), at best focus at different TF positions using trial lenses in dedicated slots in the simulator, from -1.00 to + 4.00 D, in 0.25 D step. VA was obtained from the size of the smallest letter that the patient could discriminate in each condition. Measurements were performed with the optotype at a distance of 4 m, while the patient was wearing the head-mounted SimVis2Eyes visual simulator. Proper alignment, as well as the correct interpupillary distance, was ensured by illumination with two lateral built-in LEDs sources in the device which are turned on wirelessly during adjustment. Patients were instructed to look at the stimuli with both eyes open, to move the head instead of moving their eyes, and to look through the central part of the optics of the system. Pre-operative measurements were performed with the trifocal diffractive IOL simulated for both eyes in the SimVis2Eyes clinical device. Post-operative measurements were performed with the IOL implanted in the patient, and the SimVis2Eyes correcting for the refractive error with a programmed monofocal correction.

2.5. Data analysis

TF VA curves were obtained pre-operatively with the simulated MIOLs (in both tested platforms) and post-operatively with the implanted MIOLs. The comparison between simulators and pre/post- operatively was expressed in terms of Root-Mean-Square (RMS) difference of the linearly interpolated TF curves (in a 5.00 D range). RMS of the post-pre difference TF VA curves was taken as metric for the quality of the prediction of the post-operative visual performance by the pre-operative visual simulators.

   The similarity in the shape of the TF curves was done using a cross-correlation analysis, with lag k and rho values representing the largest spike of the series when the elements of both TF

curves match exactly and the correlation coefficient, respectively. Differences between results with the different simulators, and before and after surgery were statistically analyzed using paired-samples t-test. Statistical analysis was performed using (SPSS 25 software, IBM).

3. Results

3.1. Predicted through-focus visual performance with simulated MIOLs: comparison across visual simulators

Figure 2 shows the TF VA for all 8 subjects pre-operatively, with the simulated trifocal diffractive IOL using the SLM (F2A, pink), the SimVis (F2A, green), both in the AO system platform, and using the SimVis2Eyes (F2B, orange) and SimVis (F2B, green). Black symbols represent VA (best focus for far) for a monofocal condition pre-operatively. In general, except for S#4, there is a high similarity between the TF VA curves measured with each simulator at the patient level. Blue bars in each graph represent the VA difference (SLM – SimVis, F2A; SimVis2Eyes – SimVis, F2B) at each focus position.

On average, TF VA across subjects pre-operatively showed similar trends with the simulated trifocal diffractive IOL using the SLM (Fig. 3(A), pink), and the SimVis (F3A, green), both in the AO system platform, as well as using the SimVis2Eyes (Fig. 3(B), orange), as shown in Fig. 3. The average RMS difference between the TF VA with the lenses simulated in SLM and in SimVis (measured monocularly and in monochromatic light) was 0.05 ± 0.01, and the average RMS difference between TF VA with the lenses simulated in SimVis and SimVis2Eyes (measured monocularly and in monochromatic light and binocularly and in white light) was 0.05 ± 0.01. There is not a particular trend for the magnitude of the deviation as a function of the defocus position (near, intermediate or far) or for a particular simulator providing higher VAs than the other. The cross-correlations between the TF VA curves obtained using the SimVis and the SLM and between the TF VA curves using SimVis and SimVis2Eyes were statistically high (lag k = 0, rho = 0.889 and lag k = 0, rho = 0.955, respectively).

3.2. TF VA with simulated MIOLs pre-operatively and implanted MIOLs post-operatively

Figure 4 shows the comparison between the TF VA obtained through the visual simulations with the SimVis, with the AO-based platform (Fig. 4A) or the SimVis2Eyes (Fig. 4(B)) pre-operatively (natural lens, solid lines), and post-operatively (MIOLs, dashed lines). Blue bars in each graph represent the VA difference (pre- and post-operatively).

In general, there is a good correspondence between the TF VA curves measured pre-operatively (simulated MIOL) and post-operatively (implanted MIOL), in both platforms (AO and SimVis2Eyes) for all subjects except for subject S#4. RMS difference is lower in patients with clear lens (0.06 ± 0.01 both for SimVis and for SimVis2Eyes), and higher in subjects with some degree of cataracts (S#1 catn3; S#6 catn4; S#2 catn + subcaps. posterior): 0.08 ± 0.01 for SimVis and 0.09 ± 0.01 for SimVis2Eyes. The patient with more severe degree of cataract, S#2, showed the higher RMS difference between pre- and post-surgery TF VA curves (0.39, and 0.44, with SimVis and SimVis2Eyes, respectively).

Figure 5 shows the intersubject average of the TF VA through visual simulations with SimVis (Fig. 5(A)) and SimVis2Eyes (Fig. 5(B)) before surgery (natural lens, solid lines) and after surgery (MIOLs, dashed lines). Blue bars in each graph represent the VA difference (pre- and post-operatively). The TF performance in both platforms is well captured before and after surgery. Especially in the case of clear crystalline lens patients (upper row) (paired-samples t-test: p > 0.05). TF VA after surgery in patients with cataract was higher than predicted by the simulations, while constant in the TF range (Ratio post/pre: 1.68 ± 0.12 AO-platform; 1.65 ± 0.11). In all cases, on average there is a significant cross correlation between the shape of the TF VA curves in the 4D-range for clear lens and cataract patient using the AO-based platform
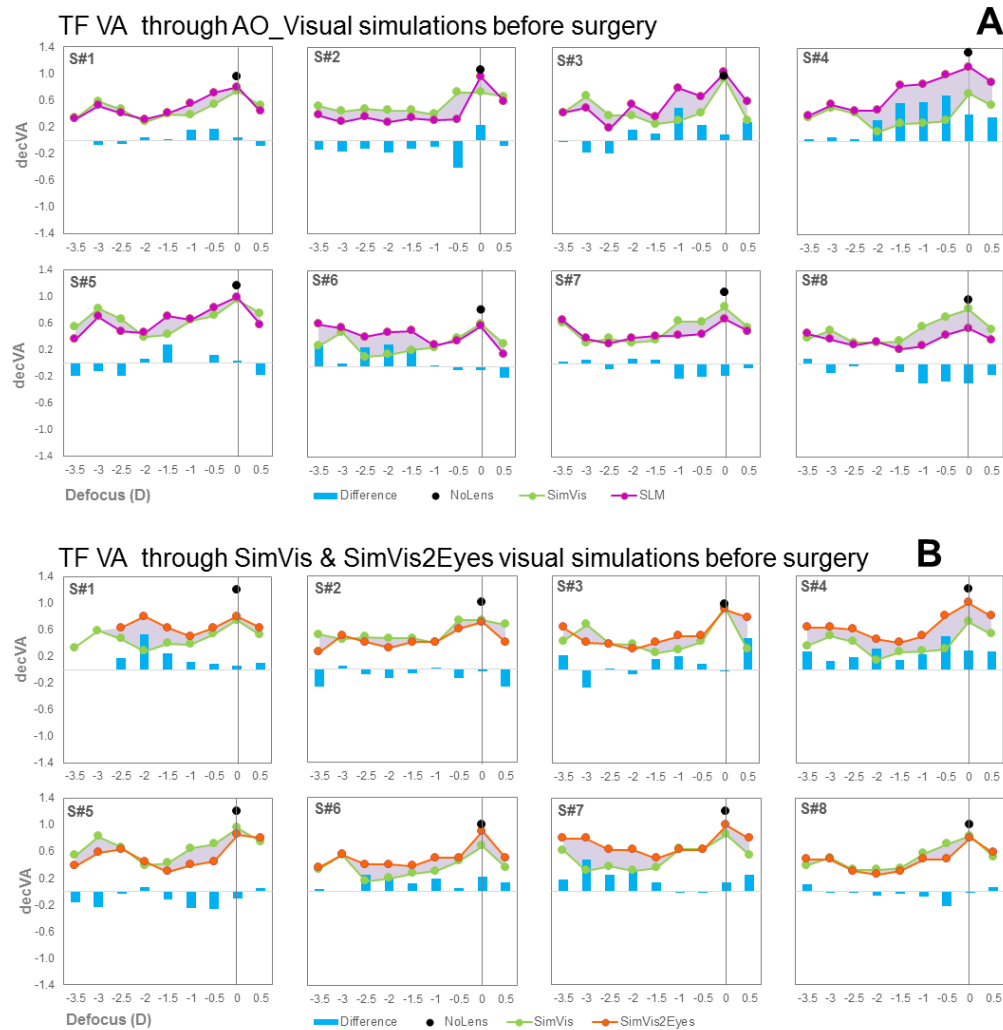
Fig. 2. TF VA obtained through simulations before surgery. (A) TF VA through AO_visual simulations (monocular, monochromatic) using the SLM (pink lines) and the SimVis (green lines), as well as VA for best subjective focus with no lens (black dots). Blue bars show the difference between SLM and SimVis. (B) TF VA through SimVis2Eyes (binocular, polychromatic) visual simulations (orange lines), and the SimVis (green lines) (monocular, monochromatic). Blue bars show the difference between SimVis and SimVis2Eyes. Black dots show the VA for best subjective focus with no lens with the SimVis2Eyes.
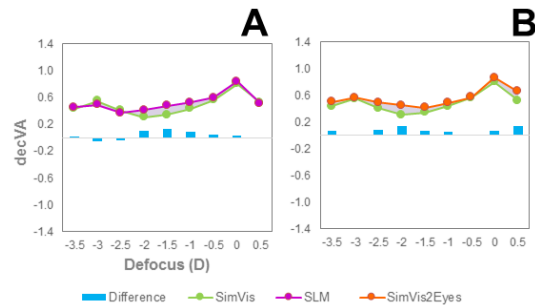
Fig. 3. Averaged TF VA obtained through simulations before surgery with all simulators. (A) TF VA pre-operatively through AO_visual simulations (monocular, monochromatic) using the SLM (pink lines) and the SimVis (green lines). (B) TF VA pre-operatively through SimVis (green lines) (monocular, monochromatic) & SimVis2Eyes (orange lines) (binocular, polychromatic) visual simulations. Blue bars in each graph represent the VA difference (SLM – SimVis; SimVis2Eyes – SimVis). The average error (standard deviation of repeated measurements, averaged across patients) was 0.058 ± 0.009 for SimVis, 0.086 ± 0.012 for SLM and 0.068 ± 0.009 for SimVis2Eyes.

(A, lag $k = 0$, rho $= 0.853$ and rho $= 0.789$) or the SimVis2Eyes (B, lag $k = 0$, rho $= 0.676$ and rho $= 0.870$), respectively.

3.3. Post-operative monochromatic-monocular TF VA vs. Polychromatic-binocular TF VA

Figure 6 shows the TF VA after surgery: (1) monochromatic (555 nm) monocular TF VA measured with the AO-based simulator (green dots) and (2) polychromatic (white light)-binocular TF VA measured with the SimVis2Eyes (orange dots) for all patients, as well as the average across patients (last panel). Measurements were performed in the two simulation platforms, although the real MIOL was already implanted and no simulation was performed. In general, the TF VA curves measured in monochromatic-monocular conditions (green curves) and polychromatic-binocular conditions (orange curves) show similar trends. On average, there is a significant cross correlation between the TF VA measured in polychromatic binocular conditions and monochromatic monocular conditions (lag $k = 0$, rho $= 0.913$). The blue bars (VA differences) are positive on average (0.07), indicating a slightly better binocular performance.
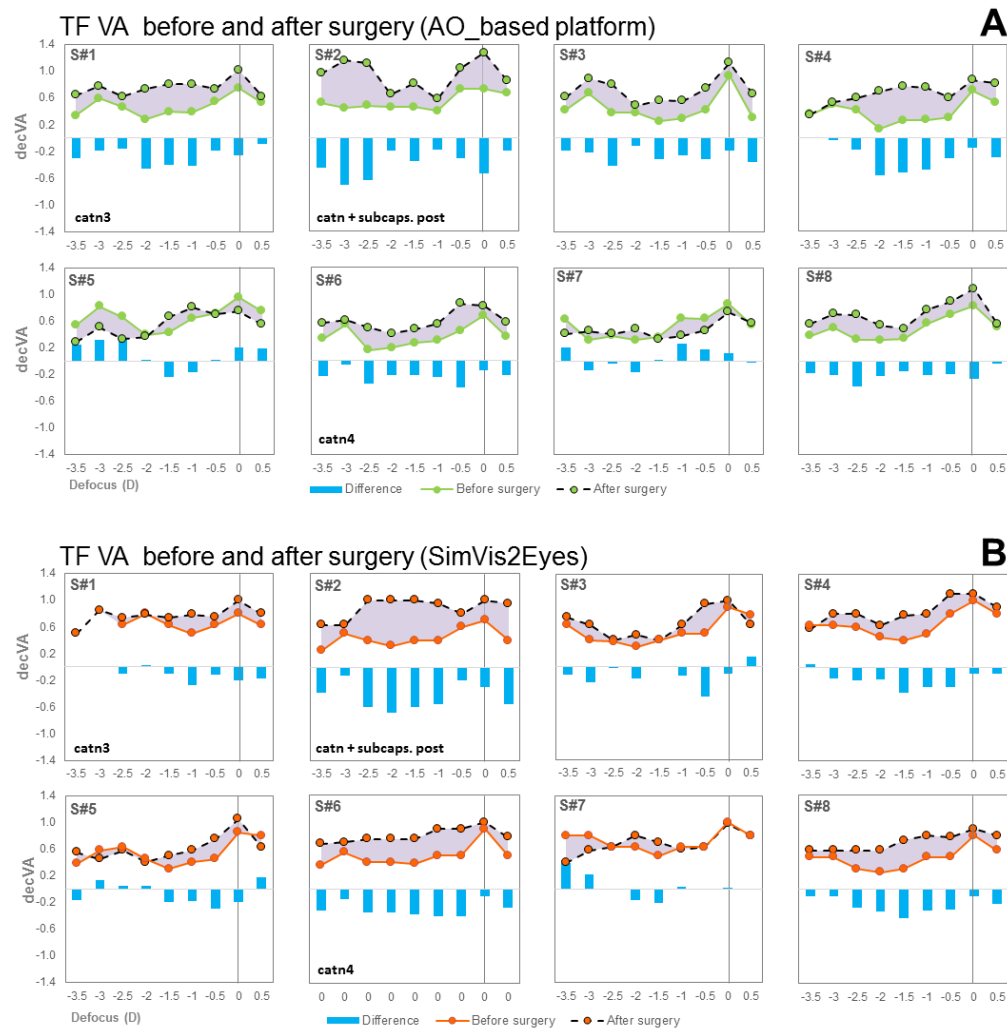
Fig. 4. TF VA obtained before and after surgery. (A) TF VA measured with the AO-based platform (monocular, monochromatic) through visual simulations before (green solid lines) and after the surgery (green dashed lines). Blue bars show differences between pre- and post-surgery measurements. (B) TF VA measured with the SimVis2Eyes platform (binocular, polychromatic) through visual simulations before (orange solid lines) and after the surgery (orange dashed lines). Blue bars show differences between pre- and post-surgery measurements. The average error (standard deviation of repeated measurements, averaged across all patients) for the simulations is indicated in Fig. 3, and for the post-operative measurements with the MIOL was 0.088 ± 0.010 in A and 0.073 ± 0.011 in B.
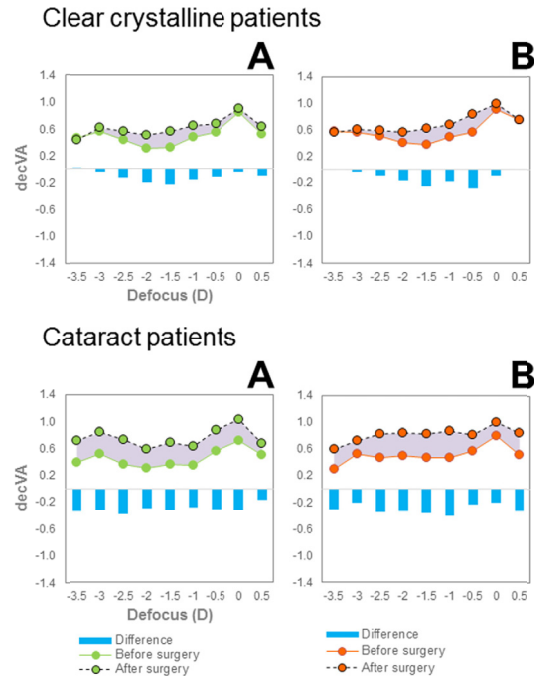
Fig. 5. Averaged TF VA obtained before and after surgery for clear crystalline lens and cataract patients. (A) TF VA measured with the AO-based platform through visual simulations (green solid lines) and after the surgery (green dashed lines). Blue bars show differences between pre- and post-surgery measurements. (B) TF VA measured with the SimVis2Eyes platform through visual simulations (orange solid lines) and after the surgery (orange dashed lines). Blue bars show differences between pre- and post-surgery measurements. The average error bar (standard deviation across patients) for the simulations is indicated in Fig. 3, and for the post-operative measurements with the MIOL in Fig. 4. The average error bar (standard deviation across patients and platforms) for SimVis2Eyes pre-operatively was 0.06 ± 0.01 and 0.05 ± 0.02, and for MIOLs post-operatively was 0.07 ± 0.01 and 0.05 ± 0.01, for clear lens and cataract patients, respectively
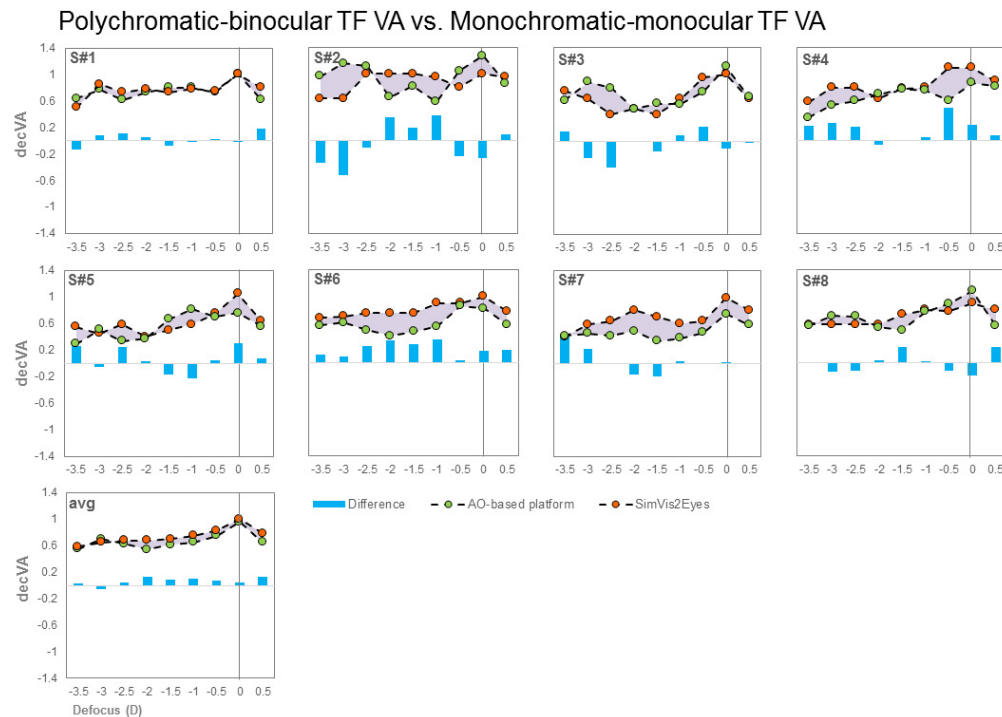
Fig. 6. Post-operative monochromatic-monocular TF VA vs. Polychromatic-binocular TF VA. TF VA after surgery, with implanted trifocal diffractive IOL, measured monocularly and with a monochromatic stimulus (green dashed lines) and binocularly and with a white-light stimulus (orange dashed lines), for each patients, and averaged across patients. Blue bars show differences between both conditions. Average errors are indicated in Fig. 4.

4. Discussion

This study presents pre-operative simulated TF visual performance in comparison with post-operative vision after implantation of a MIOL. Our averaged TF VA curves with the implanted MIOL show values of similar order of magnitude to previous reports of patients implanted with the FineVisionTrifocal IOL: CDVA:1.00 ± 0.03; DCIVA: 0.70 ± 0.10; DCNVA: 0.68 ± 0.06 in our binocular measurements with a clinical chart; CDVA: 1.00; DCIVA: 0.74; DCNVA: 0.76 in 21 eyes, measured monocularly by Poyales et al. (2016) [37]; CDVA: 1.12; DCIVA: 0.45; DCNVA: 0.89 in 30 patients, measured binocularly by Gundersen and Potvin (2017) [38]. While our average data are in good correspondence with TF visual performance reported in the literature in patients implanted with the FineVision trifocal IOL, the interesting finding in our study is the capability of the simulators to actually predict this performance pre-operatively and individually.

Visual simulators based on different active optical elements, such as DM [39], SLM [40] or IOLs in a cuvette [24], in monocular/binocular [7,23,41] configurations, are increasingly used to simulate vision through different multifocal lens designs [2,42,43]. To our knowledge, this is the first study where visual simulation of a given MIOL pre-operative is directly compared to vision post-operatively with the implanted MIOL, at the patient level. The comparison was made in patients that were implanted with diffractive trifocal lenses (the FineVision POD F, by PhysIOL), using two different simulating technologies (SLM and SimVis technology) and two different simulation platforms, an AO-based visual simulator and a binocular wearable clinical simulator, the SimVis2Eyes.

In a previous study[25], we compared TF optical (on bench) and visual quality (patients) through different simulation technologies (SLM, IOL in a cuvette, SimVis technology) in young phakic patients, and found that visual simulations in an AO system capture to a large extent the optical and visual performance obtained with projected real IOLs, as found in the current study (Fig. 3). In previous work the crystalline lens was preserved, as the real IOLs (mounted in a cuvette) were projected onto a pupil plane. Recent work suggests that the crystalline lens aberrations of a relatively young population (25-43) play a relative minor role in the performance of visual simulators replicating multifocal IOLs, at least in a SLM-based visual simulator [13].

The ultimate utility of visual simulators, no matter the technology behind, relies on their capability to allow patients to experience vision before IOL implantation, since tested IOLs are designed to replace the natural crystalline lens. In this study we compared directly pre- and post-operative TF visual quality with simulators and implanted real IOL, with clear crystalline lens and cataractous crystalline lens patients. TF visual quality pre-surgery (simulations) and after surgery (real IOL) are similar in clear crystalline lens patients (Fig. 5, upper row). This is expected, since the cornea and the multifocal pattern is a much higher contributor than the crystalline lens to pre-operative TF visual quality in clear crystalline patients. In clear crystalline patients (Fig. 5(A) & 5(B)), post-operative TF VA is slightly higher for intermediate distance than the simulated pre-operative data, probably due to scattering of the old crystalline lens, since in our previous study [23], with clear crystalline subjects no differences between simulators (SLM, SimVis and real IOL) were found. Moreover, in the case of cataractous patients, where opacities decrease TF visual quality (Fig. 5, lower row), visual simulators are still able to predict the relative TF performance post-operatively, at least up to the degree of cataract in the patients of the study, indicated by the high correspondence between the shape of the TF curves with the simulation pre-operatively and real IOLs post-operatively (p = 0.006 in the case of SimVis2Eyes). While a more comprehensive study of the role of the scattering produced by cataract (and particularly in relation to the cataract type and opacity distribution is needed) our results suggest that, at least in patients with mild cataracts, a simple conversion factor would be needed to project the expected TF performance after cataract removal from pre-operative simulation measurements.

SimVis simulation is robust, showing good correspondence between both binocular white light TF VA (measured with the clinical simulator) and monocular monochromatic TF VA (AO

visual simulator). The slightly higher VA found binocularly over monocular measurements in the majority of subjects, occurring both with SimVis before surgery (Fig. 4) and with the real MIOL after surgery (Fig. 6) can be explained by binocular summation, although this was not found to be statistically significant. It is likely that the binocular gain is counteracted by the presence of chromatic aberration in the white-illuminated target used in binocular measurements as opposed to the monochromatic stimulus of the monocular measurements. We did not attempt polychromatic measurements in the AO system, particularly as the SLM is known to be subject of chromatic artifacts [44]. Remarkably, the similarity of TF VA with SimVis and the real IOL with white targets indicate that chromatic effects are not a concern with the SimVis technology [26].

In general, we can conclude that visual simulators are able to predict the relative multifocal performance of a specific IOL design, since TF VA pre-surgery (simulated IOL) and TF VA after-surgery (real IOL) show good correspondence. In particular, in the case of a trifocal diffractive design, the predicted range for multifocality is similar to the actual relative multifocal performance after surgery. Visual simulations are useful programmable tools to predict the relative visual performance with multifocal IOLs, both in an AO environment and in a large field of view SimVis binocular device.

Funding

Acknowledgements

Disclosures

MR, SA, CB, NG, FP have no conflicting relationship; SM, CD have a patent on the technologyPCT/2014ES/070725; SM, CD, MV have financial interest on the company 2EyesVision;

References

1. W. N. Charman, "Developments in the correction of presbyopia II: surgical approaches," Ophthalmic Physiol. Opt. **34**(4), 397–426 (2014).
2. M. Vinas, C. Dorronsoro, V. Gonzalez, D. Cortes, A. Radhakrishnan, and S. Marcos, "Testing vision with angular and radial multifocal designs using Adaptive Optics," Vision Res. **132**, 85–96 (2017).
3. A. Radhakrishnan, C. Dorronsoro, and S. Marcos, "Differences in visual quality with orientation of a rotationally asymmetric bifocal intraocular lens design," J. Cataract Refractive Surg. **42**(9), 1276–1287 (2016).
4. M. Vinas, L. Sawides, P. de Gracia, and S. Marcos, "Perceptual adaptation to the correction of natural astigmatism," PLoS One **7**(9), e46361 (2012).
5. M. Vinas, C. Dorronsoro, D. Cortes, D. Pascual, and S. Marcos, "Longitudinal chromatic aberration of the human eye in the visible and near infrared from wavefront sensing, double-pass and psychophysics," Biomed. Opt. Express **6**(3), 948–962 (2015).
6. M. Vinas, C. Dorronsoro, A. Radhakrishnan, C. Benedi-Garcia, E. LaVilla, J. Schwiegerling, and S. Marcos, "Comparison of vision through surface modulated and spatial light modulated multifocal optics," Biomed. Opt. Express **8**(4), 2055–2068 (2017).
7. C. Schwarz, P. M. Prieto, E. J. Fernandez, and P. Artal, "Binocular adaptive optics vision analyzer with full control over the complex pupil functions," Opt. Lett. **36**(24), 4779–4781 (2011).
8. C. Dorronsoro, A. Radhakrishnan, J. R. Alonso-Sanz, D. Pascual, M. Velasco-Ocana, P. Perez-Merino, and S. Marcos, "Portable simultaneous vision device to simulate multifocal corrections," Optica **3**(8), 918–924 (2016).
9. P. de Gracia, C. Dorronsoro, E. Gambra, G. Marin, M. Hernandez, and S. Marcos, "Combining coma with astigmatism can improve retinal image over astigmatism alone," Vision Res. **50**(19), 2008–2014 (2010).

10. M. Vinas, P. de Gracia, C. Dorronsoro, L. Sawides, G. Marin, M. Hernandez, and S. Marcos, "Astigmatism impact on visual performance: meridional and adaptational effects," Optom. Vis. Sci. **90**(12), 1430–1442 (2013).

11. C. Schwarz, C. Canovas, S. Manzanera, H. Weeber, P. M. Prieto, P. Piers, and P. Artal, "Binocular visual acuity for the correction of spherical aberration in polychromatic and monochromatic light," J. Vis. **14**(2), 8 (2014).

12. S. Manzanera and P. Artal, "Minimum change in spherical aberration that can be perceived," Biomed. Opt. Express **7**(9), 3471–3477 (2016).

13. E. A. Villegas, S. Manzanera, C. M. Lago, L. Hervella, L. Sawides, and P. Artal, "Effect of Crystalline Lens Aberrations on Adaptive Optics Simulation of Intraocular Lenses," J. Refract. Surg. **35**(2), 126–131 (2019).

14. R. Dou and M. K. Giles, "Closed-loop adaptive-optics system with a liquid-crystal television as a phase retarder," Opt. Lett. **20**(14), 1583–1585 (1995).

15. G. D. Love, "Wave-front correction and production of Zernike modes with a liquid-crystal spatial light modulator," Appl. Opt. **36**(7), 1517–1520 (1997).

16. R. Martinez-Cuenca, V. Duran, J. Arines, J. Ares, Z. Jaroszewicz, S. Bara, L. Martinez-Leon, and J. Lancis, "Closed-loop adaptive optics with a single element for wavefront sensing and correction," Opt. Lett. **36**(18), 3702–3704 (2011).

17. Z. Zhang, Z. You, and D. Chu, "Fundamentals of phase-only liquid crystal on silicon (LCOS) devices," Light: Sci. Appl. **3**(10), e213 (2014).

18. J. Tabernero, C. Schwarz, E. J. Fernandez, and P. Artal, "Binocular visual simulation of a corneal inlay to increase depth of focus," Invest. Ophthalmol. Visual Sci. **52**(8), 5273–5277 (2011).

19. S. Marcos, L. Sawides, E. Gambra, and C. Dorronsoro, "Influence of adaptive-optics ocular aberration correction on visual acuity at different luminances and contrast polarities," J. Vis. **8**(13), 1 (2008).

20. L. Zhao, N. Bai, X. Li, L. S. Ong, Z. P. Fang, and A. K. Asundi, "Efficient implementation of a spatial light modulator as a diffractive optical microlens array in a digital Shack-Hartmann wavefront sensor," Appl. Opt. **45**(1), 90–94 (2006).

21. S. Luque and J. Pujol, "Method and system for simulating/emulating vision via intraocular devices or lenses prior to surgery," WO2012052585A1 (2012 2012).

22. W. Brezna, K. Lux, N. Dragostinoff, C. Krutzler, N. Plank, R. Tobisch, A. Boltz, G. Garhofer, R. Told, K. Witkowska, and L. Schmetterer, "Psychophysical Vision Simulation of Diffractive Bifocal and Trifocal Intraocular Lenses," Transl. Vis. Sci. Technol. **5**(5), 13 (2016).

23. M. Vinas, C. Benedi-Garcia, S. Aissati, D. Pascual, V. Akondi, C. Dorronsoro, and S. Marcos, "Visual simulators replicate vision with multifocal lenses," Sci. Rep. **9**(1), 1539 (2019).

24. J. Pujol, M. Aldaba, A. Giner, J. Arasa, and S. O. Luque, "Visual performance evaluation of a new multifocal intraocular lens design before surgery," Invest. Ophthalmol. Vis. Sci. **55**(13), 3752 (2014).

25. S. Marcos, J. S. Werner, S. A. Burns, W. H. Merigan, P. Artal, D. A. Atchison, K. M. Hampson, R. Legras, L. Lundstrom, G. Yoon, J. Carroll, S. S. Choi, N. Doble, A. M. Dubis, A. Dubra, A. Elsner, R. Jonnal, D. T. Miller, M. Paques, H. E. Smithson, L. K. Young, Y. Zhang, M. Campbell, J. Hunter, A. Metha, G. Palczewska, J. Schallek, and L. C. Sincich, "Vision science and adaptive optics, the state of the field," Vision Res. **132**, 3–33 (2017).

26. V. Akondi, C. Dorronsoro, E. Gambra, and S. Marcos, "Temporal multiplexing to simulate multifocal intraocular lenses: theoretical considerations," Biomed. Opt. Express **8**(7), 3410–3425 (2017).

27. J. D. Marsack, L. N. Thibos, and R. A. Applegate, "Metrics of optical quality derived from wave aberrations predict visual performance," J. Vis. **4**(4), 8–328 (2004).

28. D. Gatinel, C. Pagnoulle, Y. Houbrechts, and L. Gobin, "Design and qualification of a diffractive trifocal optical profile for intraocular lenses," J. Cataract Refractive Surg. **37**(11), 2060–2067 (2011).

29. D. Gatinel and Y. Houbrechts, "Comparison of bifocal and trifocal diffractive and refractive intraocular lenses using an optical bench," J. Cataract Refractive Surg. **39**(7), 1093–1099 (2013).

30. M. Vinas, A. Gonzalez-Ramos, C. Dorronsoro, V. Akondi, N. Garzon, F. Poyales, and S. Marcos, "In Vivo Measurement of Longitudinal Chromatic Aberration in Patients Implanted With Trifocal Diffractive Intraocular Lenses," J. Refract. Surg. **33**(11), 736–742 (2017).

31. R. Barraquer, L. Pinilla Cortés, M. Allende, G. Montenegro, B. Ivankovic, J. D'Antin, H. Martínez Osorio, and R. Michael, "Validation of the Nuclear Cataract Grading System BCN 10," Ophthalmic Res. **57**(4), 247–251 (2017).

32. V. Akondi, P. Perez-Merino, E. Martinez-Enriquez, C. Dorronsoro, N. Alejandre, I. Jimenez-Alfaro, and S. Marcos, "Evaluation of the True Wavefront Aberrations in Eyes Implanted With a Rotationally Asymmetric Multifocal Intraocular Lens," J. Refract. Surg. **33**(4), 257–265 (2017).

33. C. Dorronsoro, X. Barcala, E. Gambra, V. Akondi, L. Sawides, Y. Marrakchi, V. Rodriguez-Lopez, C. Benedi-Garcia, M. Vinas, E. Lage, and S. Marcos, "Tunable lenses: dynamic characterization and fine-tuned control for high-speed applications," Opt. Express **27**(3), 2085–2100 (2019).

34. W. H. Ehrenstein and A. Ehrenstein, "Psychophysical methods," in *Modern techniques in neuroscience research*, U. Windhorst and H. Johansson, eds. (Springer, 1999), pp. 1211–1240.

35. D. H. Brainard, "The Psychophysics Toolbox," Spat Vis **10**(4), 433–436 (1997).

36. J. T. Holladay, "Proper method for calculating average visual acuity," J. Refract. Surg. **13**, 388–391 (1997).

37. F. Poyales, N. Garzon, J. J. Rozema, C. Romero, and B. O. de Zarate, "Stability of a Novel Intraocular Lens Design: Comparison of Two Trifocal Lenses," J. Refract. Surg. **32**(6), 394–402 (2016).

38. K. G. Gundersen and R. Potvin, "Trifocal intraocular lenses: a comparison of the visual performance and quality of vision provided by two different lens designs," Clin. Ophthalmol. **11**, 1081–1087 (2017).

39. D. Madrid-Costa, C. Perez-Vives, J. Ruiz-Alcocer, C. Albarran-Diego, and R. Montes-Mico, "Visual simulation through different intraocular lenses in patients with previous myopic corneal ablation using adaptive optics: effect of tilt and decentration," J. Cataract Refractive Surg. **38**(5), 774–786 (2012).

40. E. J. Fernandez, P. M. Prieto, and P. Artal, "Binocular adaptive optics visual simulator," Opt. Lett. **34**(17), 2628–2630 (2009).

41. P. de Gracia, C. Dorronsoro, A. Sanchez-Gonzalez, L. Sawides, and S. Marcos, "Experimental simulation of simultaneous vision," Invest. Ophthalmol. Visual Sci. **54**(1), 415–422 (2013).

42. P. A. Piers, E. J. Fernandez, S. Manzanera, S. Norrby, and P. Artal, "Adaptive optics simulation of intraocular lenses with modified spherical aberration," Invest. Ophthalmol. Visual Sci. **45**(12), 4601–4610 (2004).

43. S. Manzanera, P. M. Prieto, D. B. Ayala, J. M. Lindacher, and P. Artal, "Liquid crystal Adaptive Optics Visual Simulator: Application to testing and design of ophthalmic optical elements," Opt. Express **15**(24), 16177–16188 (2007).

44. Z. Bouchal, V. Chlup, R. Celechovsky, P. Bouchal, and I. C. Nistor, "Achromatic correction of diffractive dispersion in white light SLM imaging," Opt. Express **22**(10), 12046–12059 (2014).